Planetary influence on the young Sun's evolution: the solar neutrino probe

Ilídio Lopes, Joseph Silk

Monthly Notices
of the
ROYAL ASTRONOMICAL SOCIETY

MNRAS **435,** 2109–2115 (2013)
Advance Access publication 2013 August 31

doi:10.1093/mnras/stt1427

Planetary influence on the young Sun's evolution: the solar neutrino probe

Ilídio Lopes[1,2]★ and Joseph Silk[3,4,5]

[1]*Centro Multidisciplinar de Astrofísica, Instituto Superior Técnico, Av. Rovisco Pais, P-1049-001 Lisboa, Portugal*
[2]*Departamento de Física, Escola de Ciencia e Tecnologia, Universidade de Évora, Colégio Luis António Verney, P-7002-554 Évora, Portugal*
[3]*Institut d'Astrophysique, UMR 7095 CNRS, Université Pierre et Marie Curie, 98bis Blvd Arago, F-75014 Paris, France*
[4]*Beecroft Institute of Particle Astrophysics and Cosmology, Department of Physics, University of Oxford, Oxford OX1 3RH, UK*
[5]*Department of Physics and Astronomy, The Johns Hopkins University, Baltimore, Homewood Campus, MD 21218, USA*

Accepted 2013 July 31. Received 2013 July 16; in original form 2013 April 10

ABSTRACT

Recent observations of solar twin stars with planetary systems, like the Sun, have uncovered that these present a peculiar surface chemical composition. This is believed to be related to the formation of earth-like planets. This suggests that twin stars have a radiative interior that is richer in heavy elements than their envelopes. Moreover, the current standard solar model does not fully agree with the helioseismology data and solar neutrino flux measurements. In this work, we find that this agreement can improve if the Sun has mass-loss during the pre-main sequence, as was previously shown by other groups. Despite this better agreement, the internal composition of the Sun is still uncertain, especially for elements heavier than helium. With the goal of inferring the chemical abundance of the solar interior, we tested several chemical compositions. We found that heavy element abundances influence the sound speed and solar neutrinos equally. Nevertheless, the carbon–nitrogen–oxygen (CNO; ^{13}N, ^{15}O and ^{17}F) neutrino fluxes are the most affected; this is due to the fact that contrarily to proton–proton (pp, pep, ^{8}B and ^{7}Be) neutrino fluxes, the CNO neutrino fluxes are less dependent on the total luminosity of the star. Furthermore, if the central solar metallicity increases by 30 per cent, as hinted by the solar twin stars observations, this new solar model predicts that ^{13}N, ^{15}O and ^{17}F neutrino fluxes increase by 25–80 per cent relative to the standard solar model. Finally, we highlight that the next generation of solar neutrino experiments will not only put constraints on the abundances of carbon, oxygen and nitrogen, but will also give some information about their radial distribution.

Key words: neutrinos – Sun: helioseismology – Sun: interior – planets and satellites: formation – planet–star interactions – stars: abundances.

1 INTRODUCTION

In recent years, significant progress has been achieved in understanding the basic principles of the formation of planetary systems around low-mass stars. Most of these findings were obtained due to high-resolution spectroscopic and photometric measurements focused on discovering earth-like planets (e.g. Udry & Santos 2007). More significantly, recent observations show evidence of a possible influence of the young planetary disc on the evolution of the host star. The most compelling evidence comes from high-resolution spectroscopic measurements of several solar twins, where it has been found that, contrary to what was previously thought, the Sun has an anomalous chemical composition when compared to identical stars without planetary systems. In fact, the Sun has a depletion of volatile and refractory elements, the effect being more pronounced for the latter, i.e. there is a 20 per cent diminution of refractory elements relatively to the volatile ones (Meléndez et al. 2009; Ramirez, Meléndez & Asplund 2009). Only 15 per cent of solar twins have a chemical composition identical to the Sun.

It is thought that the differentiation observed in the chemical composition occurs during the formation of planets in the young planetary disc. The spectroscopic observations suggest that the refractory elements are locked up in the inner planetary belt, where the earth-like planets are formed.

This is consistent with what is observed in our own Solar system and is backed up by two facts. The first is that if a depletion of 30 per cent of refractory elements is assumed to occur in the external layers of the Sun, then the amount of mass removed in the convection zone is equivalent to the combined mass of the terrestrial planets, i.e. Mercury, Venus, Earth and Mars. The second is related to the latest chemical abundance determination of the Sun, a more accurate method of spectral analysis that led to a major revision in the chemical abundances obtained from spectral absorption lines. The abundances are significantly reduced in the case of heavy chemical elements such as carbon, nitrogen, oxygen, neon, sodium and aluminium (Asplund et al. 2009). This led to a significant reduction

★ E-mail: ilidio.lopes@ist.utl.pt

in the value of the Sun's metallicity. Such variations in chemical abundances worsen the previous, possibly fortuitous, agreement of the standard solar model (SSM) with the helioseismological data and solar neutrinos, namely by increasing the difference between the sound speed profiles and by changing the location of the convection zone boundary (i.e. Turck-Chieze & Couvidat 2011; Haxton et al. 2012; Turck-Chieze & Lopes 2012). Furthermore, Serenelli, Haxton & Pena-Garay (2011) have shown that the new chemical abundances lead to a reduction of 20 per cent in the prediction of ^{8}B neutrino fluxes.

The reconciliation of the SSM (Turck-Chieze & Lopes 1993) with the helioseismic and solar neutrino data was in part re-established by several research groups, by considering alternative modifications of the evolution of the Sun (e.g. Basu & Antia 2008). Among the various attempts to solve the problem, some test the validity of the solar abundance determination (e.g. Antia & Basu 2005; Delahaye et al. 2010) and others revisit the constitutive physics of the solar model (e.g. Bahcall, Serenelli & Basu 2005) or tentatively include the impact of rotation on the evolution of the Sun (Turck-Chieze et al. 2010). The scenarios that lead to better results assume that an additional physical process occurred during the evolution of the star. The agreement was found to be best in the case of solar models that take into account mass accretion and/or mass-loss during its evolution (e.g. Guzik & Mussack 2010; Serenelli et al. 2011). Some authors (Castro, Vauclair & Richard 2007; Guzik & Mussack 2010) go a step further and consider that the depletion of heavy elements occurs in the convection zone of the star, explaining in this way the deficit in heavy elements observed in the new abundance determinations (Asplund et al. 2009), as compared with the previous ones (Grevesse & Sauval 1998). Furthermore, the evolution of the star during the gravitational contraction phase, before arriving on the main sequence, is not well known; in particular, the internal structure of the protostar is still quite uncertain. It has been suggested that, during this phase, the protostar has a radiative core rather than being fully convective, as is usually assumed (e.g. Nordlund 2009). If this is the case, there is a possibility that the radiative core of the protostar has a higher content of metals than previously assumed. These latter evolution scenarios suggest that the composition of the interior of the Sun is quite different from the composition of the convection zone. Nevertheless, by what amount the composition of the different elements decreases between the centre and the surface is not easy to justify in the presence of a quite varied set of theoretical proposals. Therefore, it is paramount that we find a way to constrain the composition inside the Sun, and if possible at different locations. The solar neutrino fluxes have the potential to discriminate between these different types of solar models, because they are produced in the core of the Sun at different locations, between the centre and 0.3 of the solar radius. Moreover, neutrino fluxes can provide a direct measure of the metallicity in the Sun's core. In this work, we address the question of whether a radial enhancement of metallicity in the core could resolve the solar abundance problem, and if so, then by what amount. In particular, we will discuss the impact of the chemical composition on the solar neutrino fluxes. We believe this could help settle the origin of such a high-metallicity radiative region and/or core, and in this way we determine the mechanism which is responsible.

2 THE ORIGIN OF CENTRAL METALLICITY

The origin of excess of metals in the Sun's interior and the mechanism responsible for their accumulation is an unresolved question: two types of scenarios could be responsible – metals were accreted from the initial host molecular cloud in the early stages of the formation of the protostar or an accretion process that occurred later on in the life of the star, when the radiative solar region was already formed; or even possibly some compromise between the two scenarios. In the latter case, the higher or lower concentration of heavy elements in the Sun's interior is very much related to the joint evolution of the host star and the planetary disc. The observational result suggests that the process of formation of the planetary disc (5 per cent of the total mass) by conservation of angular momentum is accompanied or followed by the formation of planets, which capture 90 earth masses in metals from the initial disc (Guillot 2005). It also suggests that during the planetary disc formation, ice, dust and other metal-rich materials accumulate into planets (Johnson et al. 2012; McClure et al. 2012). In the stellar disc, at a latter phase of planetary formation, the material is segregated into two components, gas and metals. The first is deposited on to the Sun, and the second is used in the formation of planets (McClure et al. 2012). The Sun develops a radiative core and a convective envelope, for which its metallicity is reduced with the accumulation of the gas from the stellar disc. In the former scenario, numerical simulations that follow the formation of the protostar from the host molecular cloud (e.g. Padoan & Nordlund 2002; Bate 2009) suggest that the protostar already possesses a radiative interior, when it arrives at the top of the Hayashi track (Wuchterl & Tscharnuter 2003). In certain cases, the protostar has a radiative core extending up to 2/3 of the solar radius. This protostar is quite different from the full convective star considered in the standard evolution scenario, just before the star starts its gravitational collapse towards the main sequence. If the protostar already has a radiative core before gravitational collapse, then this could produce a distribution of heavy elements in the Sun's core which is quite different from that used for the SSM.

3 THE SENSITIVITY OF SOLAR NEUTRINO FLUXES TO METALLICITY

The production of solar neutrinos occurs in the central region of the Sun, within a shell with a radius of $0.35\,R_{\odot}$. The precise location of the different neutrino sources depends on the specific location where the nuclear reactions occur. The neutrinos produced in the proton–proton (PP) nuclear reactions, usually known as ^{8}B, ^{7}Be, pp and pep neutrinos, are produced throughout the nuclear region, ^{8}B and ^{7}Be neutrinos are produced near the centre (5 per cent of the solar radius), and pp and pep, although produced in all the nuclear region, have a maximum flux that occurs at 10 per cent of the solar radius. The neutrinos produced in the nuclear reactions of the carbon–nitrogen–oxygen (CNO) cycle, usually referred to as ^{15}O, ^{13}N and ^{17}F, are produced within the inner shell of 10 per cent of the solar radius, with their maxima located at 5 per cent of the solar radius (Turck-Chieze & Couvidat 2011; Lopes & Turck-Chieze 2013). Almost all the nuclear reactions that produce solar neutrinos are highly sensitive to the central temperature, such T_{c}^{η} where η takes the values 10, 24, 24, 27 and 27 for ^{7}Be, ^{8}B, ^{13}N, ^{15}O and ^{17}F, respectively (Bahcall & Ulmer 1996; Lopes & Silk 2012). The exceptions are the pp and pep neutrino fluxes which have a much smaller dependence on the central temperature (η takes the values -1.1 and -2.4) due to their dependence on the total luminosity of the star.

The neutrino fluxes are the ideal tools to probe the metallicity in the Sun's core due to their sensitivity to the core plasma physics. Two reasons favour such an argument: as previously indicated, the high dependence of the nuclear reactions on the local temperature of the plasma and the dependence of the CNO cycle on the

chemical composition (including the neutrino nuclear reactions). As we will show in the next section, the solar neutrino fluxes can complement the helioseismological data diagnostics in constraining the metallicity in the nuclear region.

4 THE STANDARD SOLAR EVOLUTION

If not stated otherwise, the standard evolution model is computed starting from a young self-gravitating, full convective protostar formed during the first stages of gravitational collapse of the host molecular cloud. The current stellar codes simulate the evolution of the Sun, following the gravitational collapse of the star on the Hayashi track and the ignition of nuclear reactions in the main sequence. The calculation is stopped when the Sun arrives at its present age. In these computations, we follow the usual convention that the young protostar composition (expressed as a proportion of matter) is divided into hydrogen X_i, helium Y_i and metals Z_i, such that $X_i + Y_i + Z_i = 1$. The relative abundances of Z_i, i.e. metals, are measured from meteoric data or/and photospheric absorption lines. The former metals are known as refractory elements and the latter as volatile elements. The most important contribution to Z_i comes from the volatile elements, carbon, nitrogen and oxygen.

In the following, we choose our reference model to correspond to the SSM with updated physics, including an updated equation of state (EOS), opacities, nuclear reactions rates, and an accurate treatment of microscopic diffusion of heavy elements (Turck-Chieze & Couvidat 2011). The calculation of the solar models is done using the stellar evolution code CESAM (Morel 1997). CESAM is regularly updated with the most recent EOS and opacity coefficients (Iglesias & Rogers 1996; Iglesias & Rose 1996). The models in this work use the Hopf atmosphere and different updates on the solar composition with an adapted low-temperature opacity table. A detailed discussion on the impact of these input physics on the solar evolution can be found in Couvidat et al. (2003) and Turck-Chieze et al. (2004). The CESAM nuclear physics network uses the fusion cross-sections recommended values for the Sun (Adelberger et al. 1998, 2011), with the most recently updated nuclear reactions (Turck-Chieze & Couvidat 2011). The computation also included the appropriate screening and uses the Mitler prescription (Dzitko et al. 1995). Furthermore, the stellar evolution code also includes the microscopic diffusion of helium and other chemical elements, as described in Brun, Turck-Chieze & Morel (1998). This reference model is in full agreement with the standard picture of solar evolution (e.g. Turck-Chieze & Lopes 1993; Serenelli et al. 2009; Guzik & Mussack 2010; Turck-Chieze et al. 2010; Serenelli et al. 2011; Lopes & Turck-Chieze 2013). The solar composition used corresponds to that determined by Asplund et al. (2009). All solar models are computed by adjusting Y_i and the mixing length parameter $\alpha_{\rm MLT}$ in such a way that at the present age (4.6 Gyr) the models reproduce the solar mass, radius, luminosity and Z/X surface abundance (Turck-Chieze & Couvidat 2011).

In this computation, we use a modified version of the stellar evolution code CESAM which allows us to specify a mass-loss rate and prescribe a radial distribution of heavy metals in the Sun's radiative core. The mass-loss occurs in the upper layers of the star during a certain period before the star attains its present age. The method used to implement the mass-loss in the pre-sequence phase of the star follows a procedure identical to others (Swenson & Faulkner 1992; Guzik & Cox 1995; Morel, Provost & Berthomieu 1998; Sackmann & Boothroyd 2003). In particular, we consider that the initial mass of the star is 1.125 or 1.15 $M_\odot$ and the mass-loss rate $\dot{M}$ takes values close to $10^{-10}\,M_\odot\,{\rm yr}^{-1}$. These are identical to the values found in the literature. The proposed values are consistent with the upper limit allowed by the observed ^{7}Li lithium depletion (Boothroyd, Sackmann & Fowler 1991). Furthermore, the different values of $\dot{M}$ were chosen to improve the agreement between the sound speed of the solar model and the sound speed profile obtained from helioseismology.

We have computed two groups of solar models (cf. Tables 1 and 2): (i) solar models with an initial mass of 1.125 or 1.15 $M_\odot$, which lose mass at a rate of −0.4 to −3.0 in unities of $10^{-10}\,M_\odot\,{\rm yr}^{-1}$, the mass-loss stops when the star reaches 1 $M_\odot$ (corresponds to models α_1, β_1 and γ_1), typically, like in the case of model α_2 the mass-loss occurs from 0.5 up to 3.5 Gyr and (ii) a group of models identical to the previous ones, but which have an anomalous composition of heavy elements such as carbon, oxygen and nitrogen [corresponds to models α_i ($i = 2-5$), γ_i ($i = 2-7$) and δ_i ($i = 2-7$)]. These models have an overabundance of heavy chemical elements, such that each chemical element has an additional contribution W_i, such

Table 1. Main parameters of Z-element-modified solar models. In the table are shown the following quantities: $M_{\rm in}$ and $\dot{M}$ – the initial mass and mass-loss rate of the model; $R_{\rm BCZ}$ – radius of the base of the convective region; (A, ζ, n) – parameters of the function $W_i(r) = A\exp[-\zeta(r/{\rm R}_\odot)^n]$, which gives the anomalous composition of C, O and N. The sound speed profiles of these solar models are shown in Fig. 1 (α_1, β_1, γ_1, δ_1 and α_i with $i = 2-5$) and Fig. 2 (γ_i and δ_i with $i = 2-7$). The rightmost column indicates the line type used in Figs 1–3. Note: helioseismology data suggest that the base of the convection zone is located at 0.713 $R_\odot$ and the helium abundance in the convection zone is $Y_{\rm env} = 0.2485 \pm 0.0035$ (Basu & Antia 2004). The locations of the base of the convection zone for the SSM, α_i, β_i, γ_i and δ_i are 0.7260 $R_\odot$ (+1.82 per cent), 0.7152 $R_\odot$ (+0.3 per cent), 0.7187 $R_\odot$ (+0.8 per cent), 0.7136 $R_\odot$ (+0.08 per cent) and 0.7224 $R_\odot$ (+1.32 per cent), respectively. Similarly, the helium abundances in the envelope for the SSM, α_i, β_i, γ_i and δ_i are 0.2224 (−10.5 per cent), 0.2176 (−12.4 per cent) 0.2192 (−11.7 per cent), 0.2169 (−12.7 per cent) and 0.2210 (−11.0 per cent), respectively.

Model $M_{\rm in}$ ($M_\odot$)	$10^{-10}\dot{M}$ ($M_\odot\,{\rm yr}^{-1}$)	(A, ζ, n)	$R_{\rm BCZ}$ ($R_\odot$)	Line colour	Line type
SSM	–	–	0.7260	–	–
				Fig. 1	
α_1: 1.15	−0.5	–	0.7187	Blue	———
β_1 : –	−1.0	–	0.7152	Green	———
γ_1 : –	−0.4	–	0.7136	Magenta	———
δ_1: 1.125	−3.0	–	0.7224	Cyan	———
α_2: 1.15	−0.5	(0.3, 10, 8)	0.7152	Blue	.....
α_3 : –	–	(0.3, 10, 2)	–	Green	.....
α_4 : –	–	(0.3, 100, 2)	–	Magenta	.....
α_5 : –	–	(0.5, 200, 2)	–	Cyan	.....
				Fig. 2	
γ_1: 1.15	−0.4	–	0.7136	Repeated	———
γ_2 : –	–	(0.4, 10, 8)	–	Blue	– – –
γ_3 : –	–	(0.5, 10, 8)	–	Green	– – –
γ_4 : –	–	(0.3, 10, 2)	–	Magenta	– – –
γ_5 : –	–	(0.3, 20, 3)	–	Cyan	– – –
γ_6 : –	–	(0.3, 100, 2)	–	Red	– – –
γ_7 : –	–	(0.4, 10, 2)	–	Yellow	– – –
δ_1 1.125	−3.0	–	0.7224	Repeated	———
δ_2 : –	–	(0.4, 10, 8)	–	Blue	. – . –
δ_3 : –	–	(0.5, 10, 8)	–	Green	. – . –
δ_4 : –	–	(0.3, 10, 2)	–	Magenta	. – . –
δ_5 : –	–	(0.3, 20, 3)	–	Magenta	. – . –
δ_6 : –	–	(0.3, 100, 2)	–	Magenta	. – . –
δ_7 : –	–	(0.4, 10, 2)	–	Magenta	. – . –

Table 2. Main parameters of the solar models. In the table are shown the following quantities: $\Delta c_{\rm bcz}$ and $\Delta c_{\rm core}$ – maximum of the absolute sound speed relative difference below the base of convection zone and in the central core ($r \leq 0.3\,{\rm R}_\odot$); $Z_{\rm core}$ – Z-element abundance in the core; $\Delta\Phi(^8{\rm B})$ and $\Delta\Phi(^7{\rm Be})$ – ^{8}B and ^{7}Be total solar neutrino fluxes variation relative to SSM. The SSM corresponds to an updated solar model computed for the new estimates of solar abundances made by Asplund et al. (2009). Note: the neutrino fluxes of our SSM are $\Phi_\nu({\rm pp}) = 5.94 \times 10^{10}\,{\rm cm^2\,s^{-1}}$, $\Phi_\nu({\rm pep}) = 1.41 \times 10^8\,{\rm cm^2\,s^{-1}}$, $\Phi_\nu(^7{\rm Be}) = 4.75 \times 10^9\,{\rm cm^2\,s^{-1}}$, $\Phi_\nu(^8{\rm B}) = 5.27 \times 10^6\,{\rm cm^2\,s^{-1}}$, $\Phi_\nu(^{13}{\rm N}) = 5.32 \times 10^8\,{\rm cm^2\,s^{-1}}$, $\Phi_\nu(^{15}{\rm O}) = 4.49 \times 10^8\,{\rm cm^2\,s^{-1}}$ and $\Phi_\nu(^{17}{\rm F}) = 5.01 \times 10^6\,{\rm cm^2\,s^{-1}}$. The current solar neutrino measurements are $\Phi_{\nu,{\rm SNO}}(^8{\rm B}) = 5.05^{+0.19}_{-0.20} \times 10^6\,{\rm cm^2\,s^{-1}}$, $\Phi_{\nu,{\rm Bor}}(^8{\rm B}) = 5.88 \pm 0.65 \times 10^6\,{\rm cm^2\,s^{-1}}$, $\Phi_{\nu,{\rm Bor}}(^7{\rm Be}) = 4.87 \pm 0.24 \times 10^9\,{\rm cm^2\,s^{-1}}$ and $\Phi_{\nu,{\rm Bor}}({\rm pep}) = 1.6 \pm 0.3 \times 10^8\,{\rm cm^2\,s^{-1}}$.

Model	$\Delta c_{\rm bcz}$ (per cent)	$\Delta c_{\rm core}$ (per cent)	$Z_{\rm core}$ (–)	$\Delta\Phi(^7{\rm Be})$ (per cent)	$\Delta\Phi(^8{\rm B})$ (per cent)
SSM	1.19	0.69	0.0161	–	–
α_1	0.19	0.47	0.0155	15.32	27.44
β_1	0.51	0.27	0.0157	10.54	18.84
γ_1	0.13	0.65	0.0154	18.57	33.73
δ_1	0.86	0.31	0.0159	4.96	8.68
α_2	0.31	0.69	0.0202	15.9	27.18
α_3	0.19	0.68	0.0202	15.88	27.17
α_4	0.19	0.62	0.0202	15.70	27.20
α_5	0.19	0.64	0.0233	15.70	27.12
γ_2	0.19	0.94	0.0216	19.36	33.32
γ_3	0.23	1.02	0.0231	19.56	33.21
γ_4	0.09	0.86	0.0200	19.13	33.44
γ_5	0.08	0.87	0.0200	19.15	33.41
γ_6	0.13	0.80	0.0200	18.95	33.47
γ_7	0.09	0.93	0.0216	19.33	33.32
δ_2	1.03	0.25	0.0223	5.68	8.45
δ_3	1.07	0.31	0.0239	5.85	8.37
δ_4	0.87	0.15	0.0207	5.47	8.51
δ_5	0.86	0.12	0.0207	5.49	8.51
δ_6	0.86	0.27	0.0207	5.29	8.54
δ_7	0.86	0.11	0.0223	5.65	8.45

that $W_i(r) = A \exp\left[-\zeta (r/{\rm R}_\odot)^n\right]$. The value of A corresponds to the central increase of abundance, which is chosen to be of the order of 0.3 so as to be in agreement with the solar twin observations, and the values ζ and n are chosen to define the region where the over-abundance of heavy chemical elements occurs. The functions $W_i(r)$ were chosen initially to follow a Boltzmann distribution. Therefore, the obvious choice of n is to be equal to 2 (cf. Figs 1–3). Actually, depending on the physical processes occurring in the Sun's interior, such as the gravitational settling and diffusion of heavy elements in the radiative core, this could lead to a complicated radial distribution of chemical elements (Burgers 1969; Chapman & Cowling 1970). For reasons of completeness, n is also allowed to take on other values (cf. Table 1 and Figs 1–3).

5 DISCUSSION

Different solar models that have distinct mass-loss rates will produce a solar structure model with a sound speed profile clearly close to that favoured by helioseismology (cf. Fig. 1 and Table 2). The base of the convection zone also is close to the results obtained from helioseismological inferences (Turck-Chieze et al. 1997; Basu & Antia 2004). In our best case scenario, the sound speed difference in the radiative region just below the convection zone is smaller than 0.1 per cent (cf. Figs 1 and 2). This agreement is possible even without any specific considerations about the chemical composition.

Actually, as previously mentioned, there are several physical processes that improve the sound speed agreement between the SSM

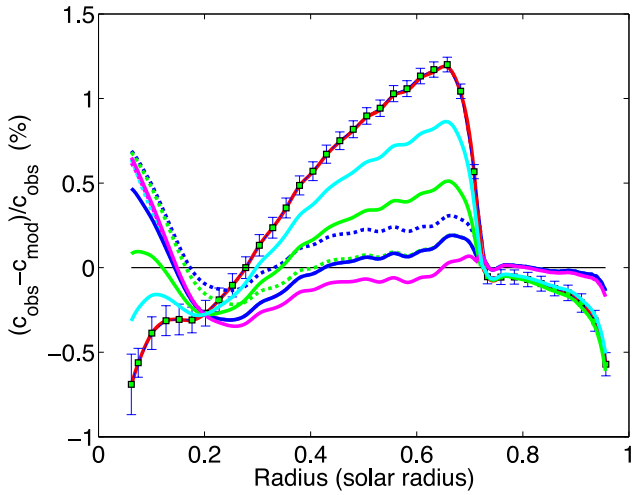

Figure 1. Relative differences between the sound speed inverted using the helioseismic data (Turck-Chieze et al. 1997; Basu et al. 2009) and the sound speed deduced from the SSM (continuous red curve with error bars). The error bars are multiplied by a factor of 10. The other curves correspond to solar models: α_1, β_1, γ_1, δ_1 and α_i with $i = 2{-}5$. The correspondence between the solar models and line type is shown in Table 1. This figure shows a set of solar models with mass-loss, with (and without) an anomalous chemical composition that improves the agreement between the solar model and the helioseismic data (cf. Fig. 3). Note: the curves corresponding to models α_i with $i = 3{-}5$ are identical (curves green dotted, cyan dotted and magenta dotted) to model α_1 (curve blue continuous) excepted in the central region ($r \leq 0.35\,{\rm R}_\odot$).

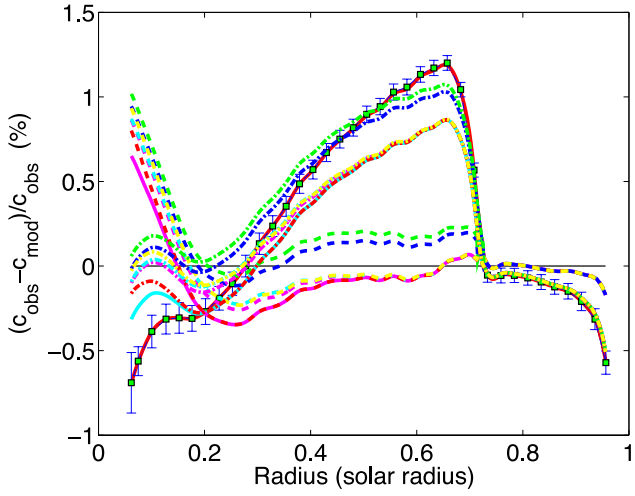

Figure 2. Relative differences between the sound speed deduced from the SSM and the sound speed obtained from helioseismic data (see Fig. 1 for details). The other curves correspond to solar models: γ_i and δ_i with $i = 2{-}7$. The correspondence between solar models and line type is shown in Table 1. This figure highlights the impact that the change in the Z-element abundance has in the sound speed (cf. Fig. 3). Note: the curves that correspond to solar models δ_i with $i = 4{-}7$ are identical to model δ_1 (cyan continuous), and the curves that correspond to solar models γ_i with $i = 4{-}7$ are identical to model γ_1 (magenta continuous), the difference between curves is only visible in the Sun's core.

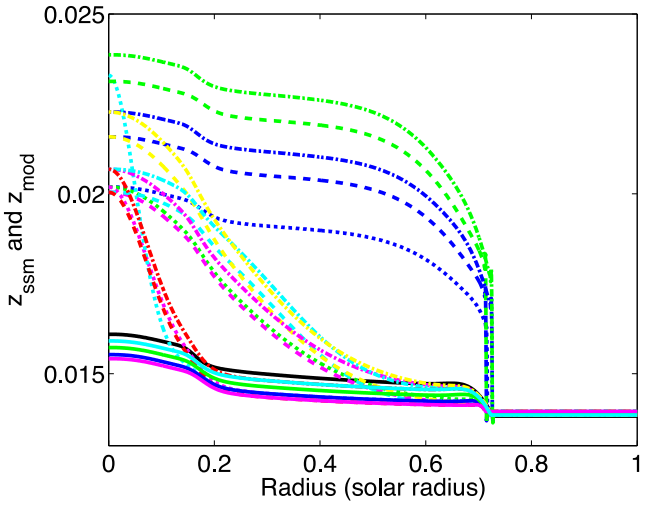

Figure 3. *Z*-element abundance profile of the present Sun computed for the SSM (using the solar mixture from Asplund et al. 2009) and other modified models. The SSM corresponds to the black curve; the other solar models are described in Table 1: the models α_1, β_1, γ_1 and δ_1 correspond to the continuous curves, and the solar models α_i ($i = 2, 5$), γ_i ($i = 2, 7$) and δ_i ($i = 2, 7$) correspond to dotted, dashed and dot–dashed lines, respectively. This figure shows anomalous *Z*-element abundances (with different dependences of the Sun's radius).

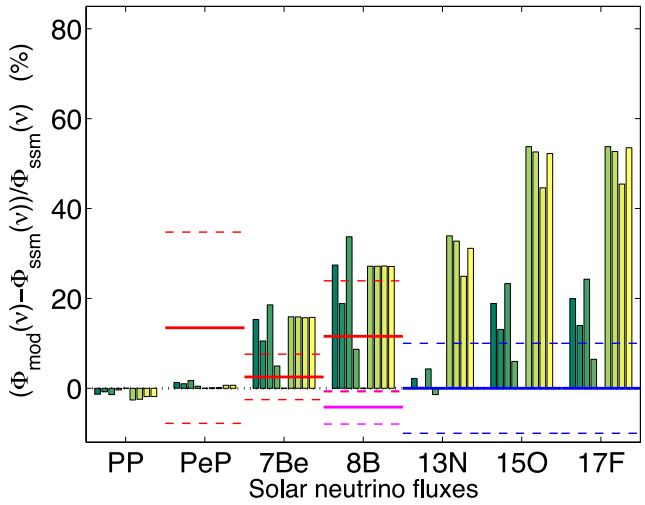

Figure 4. Percentage changes in solar neutrino fluxes for the PP chain ($pp-\nu$, $pep-\nu$, $^7Be-\nu$ and $^8B-\nu$) and CNO cycle ($^{13}N-\nu$, $^{15}O-\nu$ and $^{17}F-\nu$) relatively to SSM. For each type of neutrino fluxes the solar models are organized in a sequence of two sets (with a white space in between): models α_1, β_1, γ_1, δ_1 followed by $\alpha_2 \ldots \alpha_5$. The red horizontal lines indicate the Borexino flux neutrino measurements (with error bars) and the magenta line indicates the SNO neutrino flux measurements (with error bars). The blue horizontal lines indicate the expected precision on CNO neutrino flux measurements (see the main text). This figure shows the sensitivity of PP and CNO neutrino fluxes to changes in the mass-loss mechanisms and the composition of heavy elements of the star (compare with Fig. 1). The radial variation on the *Z*-elemental profile produces distinct variations in the fluxes of $^{13}N-\nu$, $^{15}O-\nu$ and $^{17}F-\nu$ (cf. Fig. 3).

and helioseismology, regardless of the specific chemical composition considered. Even if we consider only models with mass-loss, several solutions are possible just by fine-tuning the specific parameters such as the initial mass of the protostar, the mass-loss rate and the specific period in the evolution when the mass-loss occurs. These results are identical to those found in the literature (Guzik & Mussack 2010; Serenelli et al. 2011).

If the chemical composition of heavy elements inside the star increases by a significant amount, such as 30 per cent, as suggested by solar twin observations, the sound speed difference is reduced (cf. Fig. 1). The improvement is mainly located in the radiative region of the Sun (cf. Figs 1 and 2 and Table 2). This situation occurs for all the solar mass-loss models, and actually the result holds for quite distinct *Z*-element radial profiles (cf. Fig. 3). The base of the convective zone is not affected, if the change occurs only in *Z*-element profile (its value is fixed, cf. Table 1). This improvement can be explained by the dependence that the square of the sound speed profile has on the mean molecular weight μ, i.e. $\delta c^2/c^2 \sim \delta T/T - \delta\mu/\mu$, since μ strongly depends on *Z*. The increase of *Z* below the base of the convective zone, although less important than the mass-loss, still improves the agreement between the sound speed of the model and the helioseismological sound speed in the Sun's core. The sound speed difference δc is reduced to less than 0.1 per cent, although with a slight degradation of the agreement in the upper layers. On the other hand, the ^{7}Be and ^{8}B neutrino flux predictions come in slight disagreement with neutrino flux measurements. As mentioned previously, neutrino fluxes have the potential to distinguish between solar models with higher or lower metallicity (i.e. *Z*), in particular the CNO neutrino fluxes, by taking advantage of the high sensitivity of neutrino nuclear reaction rates to chemical composition.

The current neutrino experiments Sudbury Neutrino Observatory (SNO) and Borexino measure a value of neutrino flux of ^{8}B that corresponds to $\Phi_{\nu,\mathrm{SNO}}(^8\mathrm{B}) = 5.05^{+0.19}_{-0.20} \times 10^6\ \mathrm{cm^2\ s^{-1}}$ (Aharmim et al. 2010) and $\Phi_{\nu,\mathrm{Bor}}(^8\mathrm{B}) = 5.88 \pm 0.65 \times 10^6\ \mathrm{cm^2\ s^{-1}}$ (Bellini et al. 2010). Furthermore, the Borexino experiment also measures the ^{7}Be solar neutrino rate with an accuracy better than 5 per cent which corresponds to $\Phi_{\nu,\mathrm{Bor}}(^7\mathrm{Be}) = 4.87 \pm 0.24 \times 10^9\ \mathrm{cm^2\ s^{-1}}$, under the assumption of the Mikheyev-Smirnov-Wolfenstein large mixing angle scenario of solar neutrino oscillations (Bellini et al. 2011). Recently, the Borexino experiment made the first measurement of the pep neutrinos (Bellini et al. 2012), $\Phi_{\nu,\mathrm{Bor}}(\mathrm{pep}) = 1.6 \pm 0.3 \times 10^8\ \mathrm{cm^2\ s^{-1}}$. In Fig. 4, Φ_ν(pep), $\Phi_\nu(^8\mathrm{B})$ and $\Phi_\nu(^7\mathrm{Be})$ neutrino fluxes, among others, are presented as a variation relative to the values of the neutrino fluxes as per the SSM. In the same figure, we present the variation of modified solar models relative to the solar reference model. In solar models for which only mass-loss is considered (no variation in *Z*), the improvement in agreement between the sound speed profile and the sound speed inferred from helioseismology is followed by an increase of the difference between the ^{7}Be and ^{8}B neutrino flux measurements and the solar model. The reverse also is true. This corresponds to the sets of solar models γ_i and δ_i, respectively (cf. Tables 1 and 2 and Figs 2 and 5). The measurement in pep neutrinos is still very imprecise; therefore, no reliable constraint can be made on the physics of the solar model.

The neutrino fluxes produced in nuclear reactions of the PP chain are less sensitive to *Z* than neutrinos fluxes produced in the CNO cycle (cf. Fig. 4). The first depends mainly on the central abundance of hydrogen and helium, and only indirectly on *Z*. This is the reason why ^{7}Be and ^{8}B neutrino fluxes increase with a decrease of mass-loss rate, i.e. dependence on the total luminosity of the star is almost unaffected by the variation of chemical composition (cf. Fig. 4). Distinct *Z*-element profiles (with radial dependence) produce quite identical sound speed profiles, and ^{7}Be and ^{8}B neutrino fluxes (cf. Fig. 3). Nevertheless, there is a small improvement of the sound speed difference in the Sun's core (cf. Fig. 2 and Table 2). In particular, note that the models γ_5 and γ_7 have distinct *Z*-element

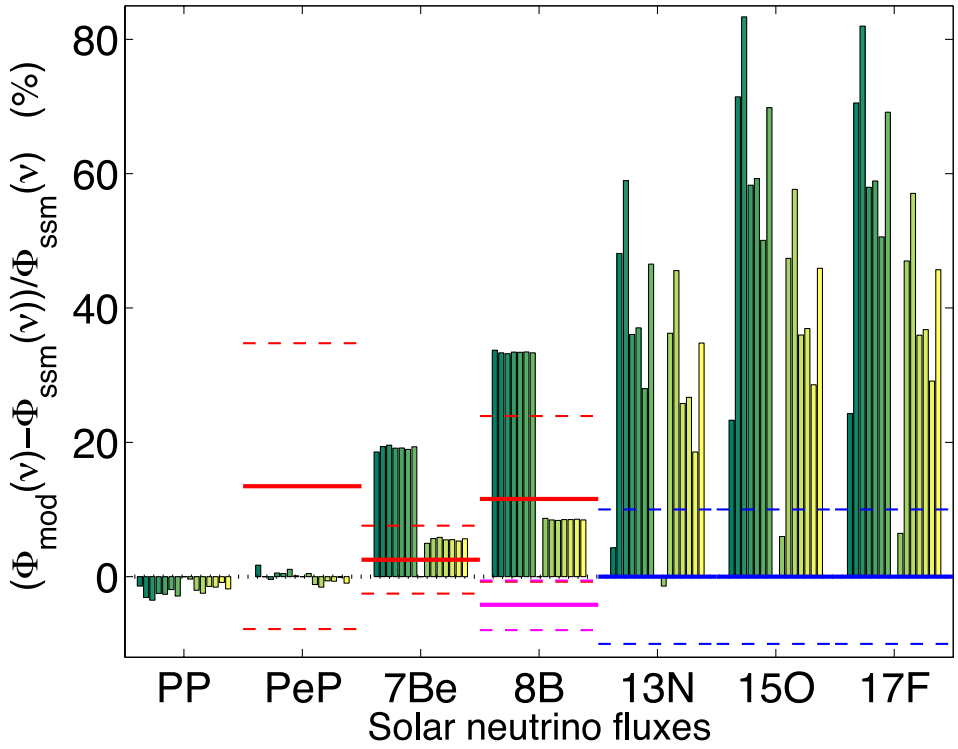

Figure 5. Percentage changes in solar neutrino fluxes for the PP chain (pp $-\nu$, pep $-\nu$, ^{7}Be $-\nu$ and ^{8}B $-\nu$) and CNO cycle (^{13}N $-\nu$, ^{15}O $-\nu$ and ^{17}F $-\nu$) relatively to SSM. The red horizontal lines indicate the Borexino flux neutrino measurements (with error bars) and the magenta line shows the SNO neutrino flux measurements (with error bars). The blue horizontal lines indicate the expected precision on the CNO neutrino flux measurements (see the main text). For each type of neutrino fluxes the solar models are organized in a sequence of two sets (with a white space in between) of models $\gamma_2 \ldots \gamma_7$ and $\delta_2 \ldots \delta_7$. Identical to the previous figure. This figure shows that the PP and CNO neutrino fluxes are equally affected for different metallicity. In the present case two sets of models are considered (cf. Fig. 2): γ_i ($i = 1-7$) – models for which the sound speed profile of the model is in very good agreement with the sound speed obtained from helioseismic data – and δ_i ($i = 1-7$) – models for which this sound speed difference is more substantial. Note that (1) the current prediction of ^{7}Be (in unities 10^9 cm^2 s^{-1}) and ^{8}B (in unities 10^6 cm^2 s^{-1}) neutrino fluxes are the following ones (the value within brackets indicates the percentage variation relative to our SSM): Serenelli et al. (2011) predict $\Phi(^7\text{Be}) = 5.00$ (+5.3 per cent) and $\Phi(^8\text{B}) = 5.58$ (+5.9 per cent) GS98 composition, and $\Phi(^7\text{Be}) = 4.56$ (−4.0 per cent) and $\Phi(^8\text{B}) = 4.59$ (−13 per cent) AGSS09 composition; Turck-Chieze et al. (2010) predict $\Phi(^7\text{Be}) = 4.72$ (−1.0 per cent) and $\Phi(^8\text{B}) = 4.72, 5.09, 4.52$ (−10.5, −3.4, −14.23 per cent); (2) the SSM in this work predicts $\Phi(^7\text{Be}) = 4.75$ (2.5 per cent experimental value measured by Borexino) and $\Phi(^8\text{B}) = 5.27$ (11.6 and −4.2 per cent experimental values measured by Borexino and SNO, respectively).

profiles (cf. Fig. 3) as well as the same sound speed profile (cf. Fig. 2), and ^{7}Be and ^{8}B neutrino fluxes, but different ^{17}F, ^{15}O and ^{13}N neutrino fluxes (cf. Fig. 5).

Although there is some uncertainty in the basic physics of the SSM, namely which physical mechanisms lead to the present structure of the Sun, like mass-loss (Guzik & Mussack 2010) or mass accretion (Serenelli et al. 2011), these types of processes act mainly by fixing the central temperature of the Sun, and by doing so affecting the sound speed profile and ^{8}B and ^{7}Be neutrino fluxes. The change in the chemical composition of heavy elements as shown in this work has a less pronounced impact on these quantities, but its impact is very distinct in CNO neutrino fluxes. Indeed, *Z*-element profiles have a quite distinct and large impact on the neutrino fluxes produced in the CNO cycle (cf. Figs 4 and 5). Two distinct signatures can be identified, the magnitude by which Z varies in the centre and the dependence of Z on the radius.

If Z increases by a fixed amount between solar models (compare models γ_2 and γ_3 in Fig. 3), then all the CNO neutrino fluxes will increase, although maintaining their relative proportionality difference (cf. Fig. 5). This is valid only if the *Z*-element profiles in these solar models are constant from the centre to the base of the convective zone.

This *Z*-element profile is almost equivalent to the one obtained with the old composition (e.g. Grevesse & Sauval 1998). However, if the *Z*-element radial profile decreases towards the surface, the neutrino sources are progressively affected, the first ones to be affected being located closest to the centre of the star. It follows that the impact is more significant for neutrinos associated with the ^{17}F, ^{15}O and ^{13}N chemical elements. The increase of Z in the core by 30 per cent produces large changes in the neutrino fluxes of ^{13}N, ^{15}O and ^{17}F. In some cases, this increases the neutrino fluxes by more than 50 per cent.

6 CONCLUSION

We found that different physical processes can adjust to the observed Sun's present luminosity leading to readjusting the internal structure of the Sun, and in particular by fixing its central temperature, in such a way that these solar models come in better agreement with the solar neutrino fluxes and helioseismic data. However, for most of the cases, the simultaneous agreement between the ^{7}Be and ^{8}B neutrino fluxes and the sound speed profile between the solar model and the real data is only possible by making a very fine tuning of the open parameters related with the physical processes considered. The typical examples are the processes related with the mass-loss or mass accretion by the star during its pre-main-sequence phase. We also found that if the metallicity content present in the Sun's interior, including the Sun's core, is quite different from the

metallicity predicted by the SSM (and also by most of the non-standard models), then the impact of these distinct Z-element profiles on the previously mentioned observed quantities is relatively small, but interestingly enough, the impact on the CNO neutrino fluxes is very pronounced. In particular, we found that a solar model with a significant increase in abundances such as carbon, oxygen and nitrogen of the order of 30 per cent, as suggested by solar twins observations (or even a higher increase of these abundances), still presents an internal structure for the present Sun quite close to the SSM. The impact of these high-metallicity profiles in the ^{7}Be and ^{8}B neutrino fluxes and helioseismology data is moderate, but its impact on the CNO neutrino fluxes is quite large. The future measurements of CNO neutrino fluxes could resolve this problem.

The new generation of neutrino experiments, such as the SNO, Borexino and low energy neutrino astrophysics (LENA), will allow a precise determination of such solar neutrino fluxes, leading to the establishment of important constraints on the composition of heavy elements in the Sun's core (Wurm et al. 2012). In particular, as pointed out by Haxton & Serenelli (2008), the future upgrade of Borexino and SNO will be able to put some constraints on the abundance of carbon and nitrogen present in the Sun's core. Furthermore, as stressed by these authors, preliminary simulations done by Chen (2007) of the SNO+ detector (Maneira 2011) suggest that after three years of operation the CNO neutrino rate should be known with an accuracy of 10 per cent (cf. Figs 4 and 5). Moreover, on the current version of the LENA project the promoters expect to improve the signal of CNO and pep neutrino fluxes relatively to the background 'noise' generated by the ^{11}C beta decays. The ^{11}C beta decays are known to be the main problem in these types of experiments. The ^{11}C background rate will be 1:8. Furthermore, Monte Carlo simulations done for the LENA detector (Wurm et al. 2011) suggest that it will be possible to find minute temporal variations (with the period window: $10^{2}-10^{9}$ s) for the amplitude of ^{7}Be neutrino flux.

If CNO neutrino flux measurements are obtained with the expected precision, we will be able to precisely determine the abundances of carbon, nitrogen and oxygen in the solar radiative region, including the deepest layers of the core. In agreement with the results obtained in this work, if the abundances of carbon, nitrogen and oxygen in the solar core are 30 per cent above the current values, then the ^{13}N, ^{15}O and ^{17}F neutrino fluxes should be 25–80 per cent above the predicted values of the current SSM.

On that account, as shown in this work, with the large improvements expected in the accuracy of future neutrino flux measurements and given the high sensitivity of neutrino fluxes to the metallicity of the Sun's interior, it should be possible to put very strong constraints on the chemical composition of the Sun.

ACKNOWLEDGEMENTS

This work was supported by grants from 'Fundação para a Ciência e Tecnologia' and 'Fundação Calouste Gulbenkian'. The authors thank the anonymous referee for the detailed analysis of the paper which has improved the contents and clarity.

REFERENCES

Adelberger E. G. et al., 1998, Rev. Mod. Phys., 70, 1265
Adelberger E. G. et al., 2011, Rev. Mod. Phys., 83, 195
Aharmim B. et al., 2010, Phys. Rev. C, 81, 55504
Antia H. M., Basu S., 2005, ApJ, 620, L129
Asplund M., Grevesse N., Sauval A. J., Scott P., 2009, ARA&A, 47, 481
Bahcall J. N., Ulmer A., 1996, Phys. Rev. D, 53, 4202
Bahcall J. N., Serenelli A. M., Basu S., 2005, ApJ, 621, L85
Basu S., Antia H. M., 2004, ApJ, 606, L85
Basu S., Antia H. M., 2008, Phys. Rep., 457, 217
Basu S., Chaplin W. J., Elsworth Y., New R., Serenelli A. M., 2009, ApJ, 699, 1403
Bate M. R., 2009, MNRAS, 392, 590
Bellini G. et al., 2010, Phys. Rev. D, 82, 33006
Bellini G. et al., 2011, Phys. Rev. Lett., 107, 141302
Bellini G. et al., 2012, Phys. Rev. Lett., 108, 51302
Boothroyd A. I., Sackmann I. J., Fowler W. A., 1991, ApJ, 377, 318
Brun A. S., Turck-Chieze S., Morel P., 1998, ApJ, 506, 913
Burgers J. M., 1969, Flow Equations for Composite Gases. Academic Press, New York
Castro M., Vauclair S., Richard O., 2007, A&A, 463, 755
Chapman S., Cowling T. G., 1970, The Mathematical Theory of Non-Uniform Gases, an Account of the Kinetic Theory of Viscosity, Thermal Conduction and Diffusion in Gases, 3rd edn. Cambridge Univ. Press, Cambridge
Chen M. C., 2007, in Wilkes J. R., ed., AIP Conf. Proc. Vol. 944, Next Generation Nucleon Decay and Neutrino Detectors: NNN06. Am. Inst. Phys., New York, p. 25
Couvidat S., Garcia R. A., Turck-Chieze S., Corbard T., Henney C. J., Jiménez-Reyes S., 2003, ApJ, 597, L77
Delahaye F., Pinsonneault M. H., Pinsonneault L., Zeippen C. J., 2010, ApJ, preprint (arXiv:1005.0423)
Dzitko H., Turck-Chieze S., Delbourgo-Salvador P., Lagrange C., 1995, ApJ, 447, 428
Grevesse N., Sauval A. J., 1998, Space Sci. Rev., 85, 161
Guillot T., 2005, Annu. Rev. Earth Planet. Sci., 33, 493
Guzik J. A., Cox A. N., 1995, ApJ, 448, 905
Guzik J. A., Mussack K., 2010, ApJ, 713, 1108
Haxton W. C., Serenelli A. M., 2008, ApJ, 687, 678
Haxton W. C., Hamish Robertson R. G., Serenelli A. M., 2012, preprint (arXiv:1208.5723)
Iglesias C. A., Rogers F. J., 1996, ApJ, 464, 943
Iglesias C. A., Rose S. J., 1996, ApJ, 466, L115
Johnson T. V., Mousis O., Lunine J. I., Madhusudhan N., 2012, ApJ, 757, 192
Lopes I., Silk J., 2012, ApJ, 752, 129
Lopes I., Turck-Chieze S., 2013, ApJ, 765, 14
Maneira J., 2011, Nucl. Phys. B – Proc. Suppl., 217, 50
McClure M. K. et al., 2012, ApJ, 759, L10
Meléndez J., Asplund M., Gustafsson B., Yong D., 2009, ApJ, 704, L66
Morel P., 1997, A&AS, 124, 597
Morel P., Provost J., Berthomieu G., 1998, ESA SP 418: SOHO 6/GONG 98 Workshop Abstract on Structure and Dynamics of the Interior of the Sun and Sun-like Stars. ESA, Noordwijk, p. 499
Nordlund A., 2009, preprint (arXiv:0908.3479)
Padoan P., Nordlund Å., 2002, ApJ, 576, 870
Ramirez I., Meléndez J., Asplund M., 2009, A&A, 508, L17
Sackmann I. J., Boothroyd A. I., 2003, ApJ, 583, 1024
Serenelli A. M., Basu S., Ferguson J. W., Asplund M., 2009, ApJ, 705, L123
Serenelli A. M., Haxton W. C., Pena-Garay C., 2011, ApJ, 743, 24
Swenson F. J., Faulkner J., 1992, ApJ, 395, 654
Turck-Chieze S., Couvidat S., 2011, Rep. Prog. Phys., 74, 6901
Turck-Chieze S., Lopes I., 1993, ApJ, 408, 347
Turck-Chieze S., Lopes I., 2012, Res. Astron. Astrophys., 12, 1107
Turck-Chieze S. et al., 1997, Sol. Phys., 175, 247
Turck-Chieze S., Couvidat S., Piau L., Ferguson J., Lambert P., Ballot J., Garcia R. A., Nghiem P., 2004, Phys. Rev. Lett., 93, 211102
Turck-Chieze S., Palacios A., Marques J. P., Nghiem P. A. P., 2010, ApJ, 715, 1539
Udry S., Santos N. C., 2007, Annu. Rev. Astron. Astrophys., 45, 397
Wuchterl G., Tscharnuter W. M., 2003, A&A, 398, 1081
Wurm M. et al., 2011, Phys. Rev. D, 83, 32010
Wurm M. et al., 2012, Astropart. Phys., 35, 685

This paper has been typeset from a TEX/LATEX file prepared by the author.